Available online at www.sciencedirect.com
SCIENCE @ DIRECT®
Earth and Planetary Science Letters 216 (2003) 441–455
www.elsevier.com/locate/epsl

Frontiers

Mercury: the enigmatic innermost planet

Sean C. Solomon *

Department of Terrestrial Magnetism, Carnegie Institution of Washington, Washington, DC 20015, USA

Received 3 July 2003; received in revised form 26 September 2003; accepted 29 September 2003

Abstract

The planet Mercury, a difficult object for study by astronomical observation and spacecraft exploration alike, poses multiple challenges to our general understanding of the inner planets. Mercury's anomalously high uncompressed density implies a metal fraction of 60% or more by mass, an extreme outcome of planetary formational processes common to the inner solar system. Whether that outcome was the result of chemical gradients in the early solar nebula or removal by impact or vaporization of most of the silicate shell from a differentiated protoplanet can potentially be distinguished on the basis of the chemical composition of the present crust. Our understanding of the geological evolution of Mercury and how it fits within the known histories of the other terrestrial planets is restricted by the limited coverage and resolution of imaging by the only spacecraft to have visited the planet. The role of volcanism in Mercury's geological history remains uncertain, and the dominant tectonic structures are lobate scarps interpreted as recording an extended episode of planetary contraction, issues that require global imaging to be fully examined. That Mercury has retained a global magnetic field when larger terrestrial planets have not stretches the limits of standard hydromagnetic dynamo theory and has led to proposals for a fossil field or for exotic dynamo scenarios. Hypotheses for field generation can be distinguished on the basis of the geometry of Mercury's internal field, and the existence and size of a fluid outer core on Mercury can be ascertained from measurements of the planet's spin axis orientation and gravity field and the amplitude of Mercury's forced librations. The nature of Mercury's polar deposits, suggested to consist of volatile material cold-trapped on the permanently shadowed floors of high-latitude impact craters, can be tested by remote sensing of the composition of Mercury's surface and polar atmosphere. The extremely dynamic exosphere, which includes a number of species derived from Mercury's surface, offers a novel laboratory for exploring the nature of the complex and changing interactions among the solar wind, a small magnetosphere, and a solid planet. Recent ground-based astronomical measurements and several new theoretical developments set the stage for the in-depth exploration of Mercury by two spacecraft missions within the coming decade.
© 2003 Elsevier B.V. All rights reserved.

Keywords: Mercury; planet formation; planetary composition; planetary geology; magnetic fields

1. Introduction

By many measures Mercury is an intriguingly odd member of the planetary family [1]. It is the smallest of the terrestrial planets, but its density (corrected for self-compression) and by inference

* Tel.: +1-202-478-8850; Fax: +1-202-478-8821.
E-mail address: scs@dtm.ciw.edu (S.C. Solomon).

0012-821X/03/$ – see front matter © 2003 Elsevier B.V. All rights reserved.
doi:10.1016/S0012-821X(03)00546-6

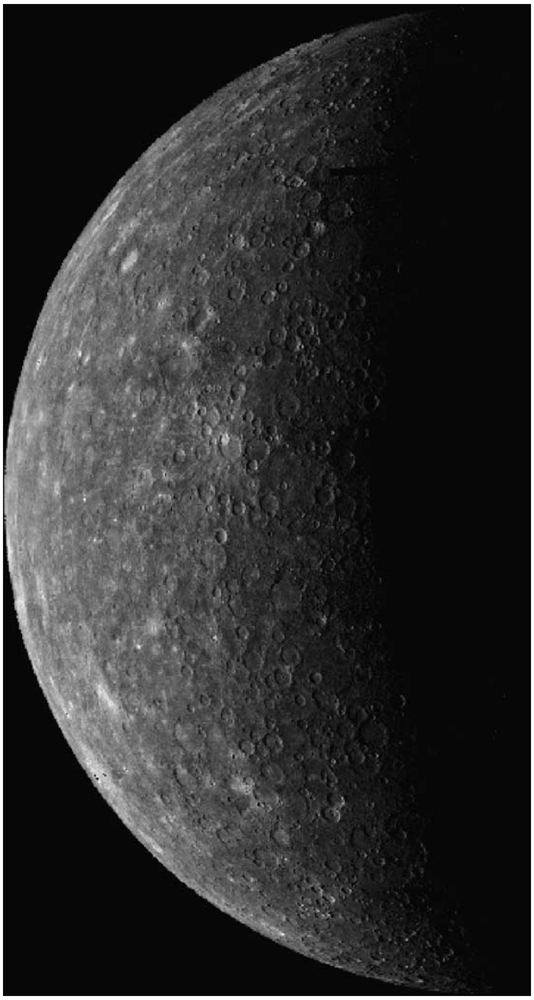

Fig. 1. Mosaic of images of Mercury obtained by the Mariner 10 spacecraft on the incoming portion of its first flyby of Mercury [102]. Mercury has a radius of 2440 km and a mass equal to 0.055 Earth masses.

its mass fraction of metal are the highest of any planet in the solar system. Its ancient surface (Fig. 1) suggests that internal geological activity ceased earlier than on any other terrestrial planet, yet it retains a global magnetic field of internal origin. As the closest planet to the Sun, Mercury displays the largest range in diurnal temperature in the solar system, but the floors of its polar craters remain sufficiently cold to trap highly volatile species. It is the only solar system body locked in a spin–orbit resonance where the ratio of orbital period to spin period is precisely 3:2 (unlike the more common 1:1 ratio, as for the Moon). Mercury's atmosphere is both the most tenuous and the most strongly variable among the terrestrial planets and the only atmosphere in which such crustally derived elements as sodium, potassium, and calcium are major constituents.

A further context in which to regard Mercury's unusual attributes is provided by the recent discovery of planets and planetary systems in orbit about other stars [2]. While the extrasolar planets documented to date are all analogues to the gas-giant planets of our solar system, the orbital parameters of Mercury fall within those of known extrasolar planets (Fig. 2), and Mercury provides our nearest laboratory for studying planetary system processes in the vicinity of a host star. Further, a variety of efforts are under way to detect and characterize extrasolar Earth-like planets [3], and Mercury will provide a relevant point of comparison with those less than 1 AU from their parent star.

Mercury is, however, a difficult object for study. Earth-based astronomical observations must contend with the fact that Mercury is never far from the Sun in the sky. Mercury is a forbidden target of the Hubble Space Telescope and presumably of other space imaging systems for

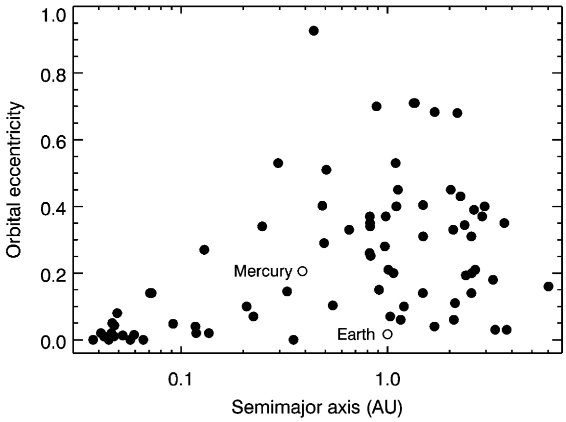

Fig. 2. Orbital characteristics of extrasolar planets compared with those of Mercury and Earth. Shown are all extrasolar planet candidates with $M \sin i < 10\ M_J$ and with published radial velocity measurements [2], where M is the planet mass, i is the angle between the planet's orbital plane and the line linking the Earth and the parent star, and M_J is the mass of Jupiter [103].

which direct observations near the Sun must be avoided. Mercury poses severe thermal and dynamical challenges to observation by spacecraft, and to date the planet has been visited only by Mariner 10, which flew by Mercury three times in 1974–1975.

Two spacecraft missions are now being readied to return to Mercury with suites of sophisticated instruments to carry out remote sensing and in situ measurements. The MESSENGER (MErcury Surface, Space ENvironment, GEochemistry, and Ranging) mission [4–6], developed under the Discovery Program of the U.S. National Aeronautics and Space Administration, is scheduled to be launched in 2004, to fly by Mercury in 2007 and 2008, and to orbit Mercury for one year beginning in 2009. The BepiColombo mission, under development by the European Space Agency and the Institute of Space and Astronautical Science in Japan, will include two orbiting spacecraft and the option of a landed package and will launch as early as 2011 [7–9]. In part because of these upcoming missions, and in part the result of improvements in astronomical technology and methodology, the planet Mercury has been the object of renewed theoretical and observational interest.

The scientific objectives of the MESSENGER mission hint at the broader importance of Mercury to our general understanding of the processes that governed the formation and evolution of the inner planets. MESSENGER was designed to address six broad scientific questions [4]:

What planetary formational processes led to the high metal/silicate ratio in Mercury?

What is the geological history of Mercury?

What are the nature and origin of Mercury's magnetic field?

What are the structure and state of Mercury's core?

What are the radar-reflective materials at Mercury's poles?

What are the important volatile species and their sources and sinks on and near Mercury?

These questions, also objectives of the BepiColombo mission [7,10], provide a framework for laying out the principal issues to be addressed by spacecraft observations at Mercury as well as the most recent progress that has been made toward sharpening these issues and their interconnections in anticipation of the forthcoming missions.

2. Mercury's bulk composition

Mercury's uncompressed density (about 5.3 Mg/m^3), the highest of any planet, has long been taken as evidence that iron is the most abundant contributor to the bulk composition. Interior structure models in which a core has fully differentiated from the overlying silicate mantle indicate that the core radius is approximately 75% of the planetary radius and the fractional core mass about 60% if the core is pure iron; still larger values are possible if the core has a light element such as sulfur alloyed with the iron [11]. Such a metallic mass fraction is at least twice that of the Earth, Venus, or Mars.

Calculations of dynamically plausible scenarios for the accretion of the terrestrial planets permit a wide range of outcomes for Mercury. Given an initial protoplanetary nebular disk of gas and dust, planetesimals accrete to kilometer size in 10^4 years [12] and runaway growth of planetary embryos of Mercury to Mars size accrete by the gravitational accumulation of planetesimals in 10^5 years [13]. During runaway growth, Mercury-size bodies can experience substantial migrations of their semimajor axes [14]. Further, each of the terrestrial planets probably formed from material originally occupying a wide range in solar distance, although some correlation is expected between the final heliocentric distance of a planet and those of the planetesimals from which it formed [14,15].

Three explanations for the high metal fraction of Mercury have been put forward. The first invokes differences in the response of iron and silicate particles to aerodynamic drag by nebular gas to achieve fractionation at the onset of planetesimal accretion [16]. The second and third explanations invoke processes late in the planetary accretion process, after the Mercury protoplanet had differentiated silicate mantle from metal core. In one, the high metal content of Mercury is attributed to preferential vaporization of silicates by radiation from a hot nebula and removal by a strong solar wind [17,18]. In the other, selective removal of silicate occurred as a result of a giant impact [14,19].

These three hypotheses lead to different predictions for the bulk chemistry of the silicate fraction of Mercury [20]. Under the giant impact hypothesis, the residual silicate material on Mercury would be dominantly of mantle composition. The FeO content would reflect the oxidation state of the material from which the protoplanet accreted, but the loss of much of the original crust would deplete Ca, Al, and alkali metals without enriching refractory elements. The vaporization model, in contrast, predicts strong enrichment of refractory elements and depletion of alkalis and FeO [18]. Under both of these hypotheses, the present crust should represent primarily the integrated volume of magma produced by partial melting of the relic mantle. Under the aerodynamic sorting proposal [16], the core and silicate portions of Mercury can be prescribed by nebular condensation models, suitably weighted by solar distance, except that the ratio of metal to silicate is much larger [20]. This hypothesis permits a thick primordial crust, i.e., one produced by crystal–liquid fractionation of a silicate magma ocean. Determining the bulk chemistry of the silicate portion of Mercury thus offers an opportunity to discern those processes operating during the formation of the inner solar system that had the greatest influence on producing the distinct compositions of the inner planets.

Present information on the chemistry and mineralogy of the surface of Mercury, however, is too limited to distinguish clearly among the competing hypotheses. Ground-based reflectance spectra at visible and near-infrared wavelengths do not show a consistent absorption feature near 1 μm diagnostic of Fe^{2+} [21], limiting the average FeO content to be less than about 3–4 wt% [22]. Very reduced compositions comparable to enstatite achondrite meteorites with less than 0.1% FeO are compatible with Mercury's reflectance, although a generally red spectral slope is thought to be the result of nanophase iron metal, altered by space weathering from silicates originally con-

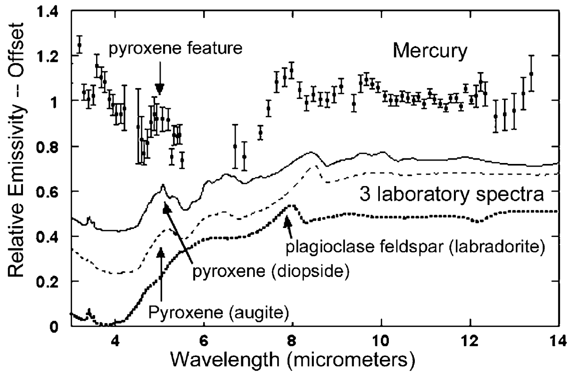

Fig. 3. Mid-infrared spectra of Mercury [24] compared with those for three laboratory samples. The peak near 5 μm matches features attributable to pyroxene, and the peak near 8 μm matches spectral characteristics of plagioclase feldspar [1].

taining a few percent FeO [23]. Earth-based mid-infrared observations show emission features (Fig. 3) consistent with the presence of both calcic plagioclase feldspar containing some sodium and very-low-FeO pyroxene; variations in spectral features with Mercury longitude indicate that surface mineralogical composition is spatially heterogeneous [24]. Mature lunar highland anorthosite soils are regarded as good general spectral analogues to Mercury surface materials [25].

On the basis of the low FeO content of Mercury's surface materials inferred from Earth-based spectra and Mariner 10 color images, surface units interpreted as volcanic in origin are thought to average no more than about 3% FeO by weight [26]. On the grounds that the solid/liquid partition coefficient for FeO during partial melting of mantle material is near unity, the mantle FeO abundance has been inferred to be comparable [26]. This deduction, together with a general increase in bulk silicate FeO content with solar distance for the terrestrial planets and the eucrite parent body, has been taken to suggest both that the inner solar nebula displayed a radial gradient in FeO and that Mercury was assembled dominantly from planetesimals that formed at solar distances similar to that of Mercury at present [26].

Were samples from Mercury to be recognized in the world's meteorite collections, of course, it would be possible to obtain information on isotopic and trace element abundances in crustal materials that cannot be measured from an orbiting spacecraft. The ejection and transport of meteorites from Mercury to Earth is dynamically feasible, although the probability of delivery is lower than for meteorites from Mars by at least two orders of magnitude [27]. It has been suggested that a recently recovered basaltic achondrite having an oxygen isotopic signature distinct from the eucrite parent body [28] may have come from Mercury [29]. This suggestion is difficult to test at present, but the high FeO content (21 wt%) of the meteorite [28] would make this object unrepresentative of the global surface composition.

Substantial progress on understanding the composition of Mercury must await remote sensing by orbiting spacecraft and in situ measurement of the chemistry of surface materials [9]. Instruments on an orbiter that can provide direct chemical information include γ-ray [30], X-ray [31], and neutron [32] spectrometers. Information on surface mineralogy can be obtained from reflectance spectrometry [33] and color imaging [34,35]. Also important to an assessment of bulk composition and formation hypotheses would be an estimate of the thickness of Mercury's crust. The thickness can be estimated by a combined analysis of gravity and topography measurements if such data are sensitive to variations on horizontal scales of several hundred kilometers and greater [36,37]. An upper bound on crustal thickness can also be obtained from isostatically compensated long-wavelength topographic variations, on the grounds that the temperature at the base of the crust cannot be so high that variations in crustal thickness are removed by viscous flow on timescales shorter than the age of the crust [38].

3. Mercury's geological history

A generalized geological history of Mercury has been developed from Mariner 10 images [39]. The 45% of Mercury's surface imaged by Mariner 10 can be divided into four major terrains. Heavily cratered regions have an impact crater density suggesting that this terrain records the period of heavy bombardment that ended about 3.8 billion years ago on the Moon [35]. Intercrater plains, the most extensive terrain type, were emplaced over a range of ages during the period of heavy bombardment. Hilly and lineated terrain occurs antipodal to the Caloris basin, at 1300 km diameter the largest and youngest [35] known impact structure on Mercury, and is thought to have originated at the time of the Caloris impact by the focusing of impact-generated shock waves. Smooth plains, the youngest terrain type, cover 40% of the area imaged by Mariner 10, are mostly associated with large impact basins, and are in a stratigraphic position similar to that of the lunar maria. On the basis of the areal density of impact craters on the portion of Mercury's surface imaged by Mariner 10, as well as the scaling of cratering flux from the Moon to Mercury, smooth plains emplacement may have ended earlier on Mercury than did mare volcanism on the Moon [35].

The role of volcanism in Mercury's geological history is uncertain. Both volcanic and impact ejecta emplacement mechanisms have been suggested for the intercrater and smooth plains, and the issue remains unresolved because no diagnostic morphological features capable of distinguishing between the two possibilities are clearly visible at the typical resolution of Mariner 10 images [40]. Ground-based infrared and millimeter observations of Mercury have been interpreted as indicating a generally basalt-free surface and thus a magmatic history dominated either by intrusions or by eruptions of only low-FeO (FeO plus TiO_2 less than 6% by weight) lavas [41]. Recalibration of Mariner 10 color images and reprojection using color parameters sensitive to iron content, soil maturity, and opaque mineral abundances indicate that geological units are distinguishable on the basis of color [42]. In particular, the correlation of color boundaries with lobate boundaries of smooth plains previously mapped from Mariner 10 images (Fig. 4) supports the inference that the plains units are volcanic deposits compositionally distinct from underlying older crustal material [42].

Mercury's tectonic history is unlike that of any other terrestrial planet. The most prominent tectonic features on the surface are lobate scarps

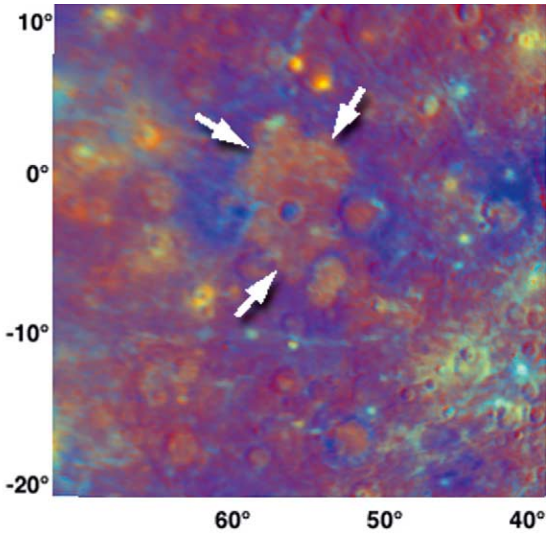

Fig. 4. Color composite mosaic of a portion of Mercury's surface [42]. The red component is the inverse of the opaque index (increasing redness indicates decreasing opaque mineralogy), the green component is a function of the combined ferrous iron content and soil maturity, and blue is the ratio of brightness in ultraviolet to that in orange light. Smooth plains units exhibit a distinct color (reddish on this image) from their surroundings and embaying boundaries (arrows) consistent with material emplaced as a fluid flow. Both characteristics support the hypothesis that the plains are volcanic in origin.

(Fig. 5), 20–500 km in length and hundreds of meters to several kilometers in height [43]. On the basis of their asymmetric cross-sections, rounded crests, sinuous but generally linear to arcuate planforms, and transection relationships with craters, the scarps are interpreted to be the surface expression of major thrust faults [39]. Because the scarps are more or less evenly distributed over the well-imaged portion of the surface and display a broad range of azimuthal trends, they are thought to be the result of global contraction of the planet. From the lengths and heights of the scarps, and from simple geometric fault models or fault length–displacement relationships, the inferred 0.05–0.10% average contractional strain if extrapolated to the full surface area of the planet would be equivalent to a decrease of 1–2 km in planetary radius [39,43]. Scarp formation postdated the intercrater plains, on the grounds that no scarps are embayed by such plains material, and extended until after emplacement of smooth plains units [39].

This estimate of global contraction poses a potentially strong constraint on models for cooling of Mercury's interior. Thermal history calculations that incorporate parameterized core and mantle convection as well as the generation and upward transport of mantle partial melt [44] indicate that models consistent with 0.05–0.10% surface contraction since the end of heavy bombardment are limited to those with a mantle rheology appropriate to anhydrous conditions, modest concentrations of heat-producing elements, and a significant fraction of a light alloying element (e.g., S) in the core to limit inner core solidification (Fig. 6). A larger range of models is permitted if the unseen hemisphere of Mercury experienced greater contraction or if other modes of deformation than lobate scarp formation accommodated additional contractional strain [45]. A further constraint on thermal models may come from estimates of the depth of faulting that accompanied scarp formation. Modeling of the topographic profile across Mercury's longest known scarp (Fig. 5) yields an inferred depth of faulting of 35–40 km, and from an estimate of the

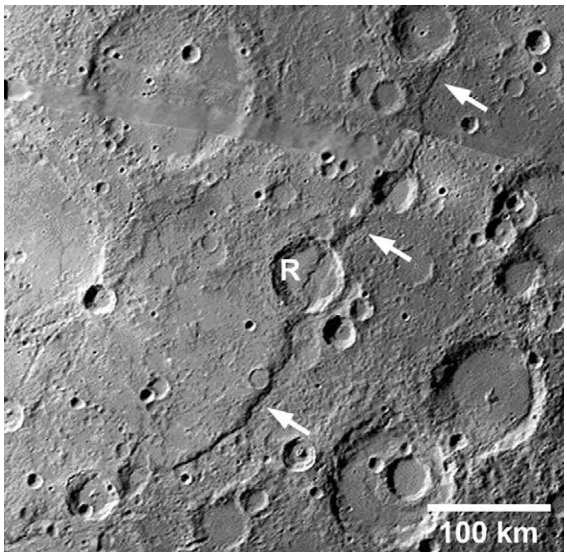

Fig. 5. Mariner 10 mosaic of Discovery Rupes (arrows), at 550 km the longest known lobate scarp on Mercury [43]. The crater Rameau (R), transected by the scarp, is 60 km in diameter.

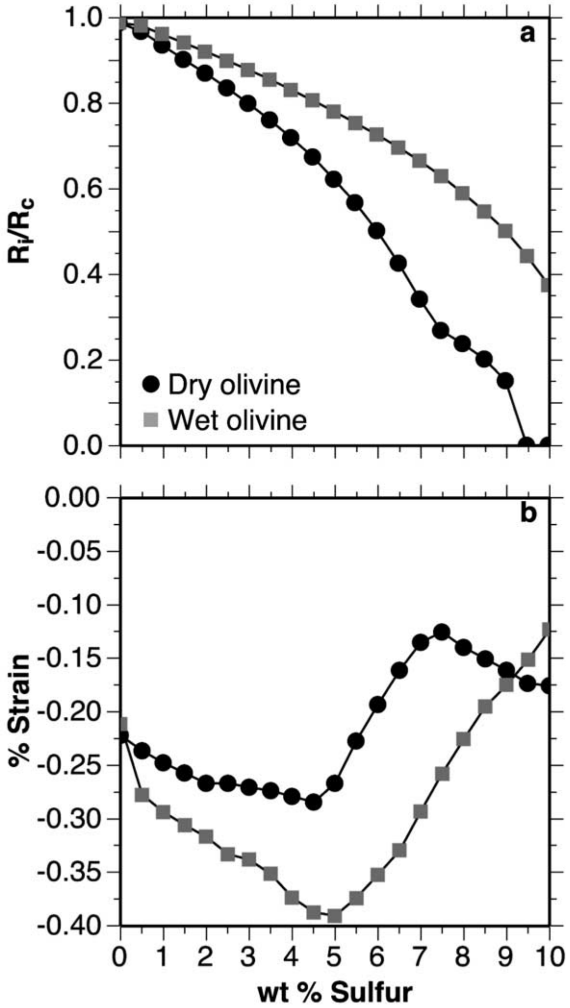

Fig. 6. Present inner core radius (as a fraction of outer core radius) and surface contractional strain accumulated since the end of heavy bombardment for a suite of thermal history models for Mercury [44]. The models shown differ in the average sulfur composition of the core and in whether the flow law governing convection in the mantle is that for anhydrous or water-saturated olivine.

temperature limiting brittle behavior a thermal gradient may be derived [46], although the age appropriate to that estimate and the degree to which it is representative of the global average gradient at that time are not known.

Recent ground-based imaging has yielded information on the hemisphere of Mercury not viewed by Mariner 10. Optical to near-infrared images of the sunlit portion of Mercury have been made by two groups utilizing short-exposure, high-definition techniques [47–49]. Resolution of the best such images approaches 200 km, and both bright and dark features appear in common locations on those portions of the surface imaged with both methods [50]. Dark features are thought to be plains [50], and a majority of the bright features are likely to be young rayed craters, which have comparable densities on Mercury's two hemispheres [49]. Radar images at substantially higher resolution have been obtained of a number of radar-bright features on the side of Mercury not imaged by Mariner 10 [51,52]. At the highest resolution these features appear to be of impact origin [52], including one previously speculated to be a volcanic construct on the basis of earlier radar images of coarser resolution [51].

To make a substantial improvement in our knowledge of the full geological history of Mercury, global multicolor imaging of the surface from an orbiting spacecraft will be required. Average resolution should be significantly better than that typical of Mariner 10 images, and a capability for targeted high-resolution imaging is desirable [35]. Topographic information would aid in landform identification and could be obtained from an altimeter [5], stereo photogrammetry [53], or preferably a combination of the two methods.

4. Mercury's magnetic field

Mercury's intrinsic magnetic field, discovered by Mariner 10 [54], has a dipole component nearly orthogonal to Mercury's orbital plane and a moment near 300 nT-R_M^3 (about 0.1% of Earth's dipole moment), where R_M is Mercury's mean radius [55]. The origin of this field, however, is not understood [56]. Mercury's magnetic field cannot be externally induced, on the grounds that the measured planetary field is far greater in magnitude than the interplanetary field [55]. The dipole field could be a remanent or fossil field acquired during lithospheric cooling in the presence of an internal or external field [57,58], or it could be the product of a modern core dynamo [56,59].

Permanent magnetization from an external source has been discounted on the grounds that a thick shell of coherently magnetized material is needed to match the observed dipole moment, and the lithosphere of Mercury would not have been able to cool and thicken sufficiently in the time interval during which strong solar or nebular fields were present [59]. Permanent magnetization from an internal source has been questioned on the grounds that a high specific magnetization of the shell and a characteristic interval between field reversals much longer than on Earth are both required [59].

The hypothesis that Mercury's internal field is remanent is receiving renewed attention after the discovery of strongly magnetized regions in the crust of Mars [60]. Mars may not be a good analogue to Mercury in all respects, because the potential magnetic carriers on Mars are iron-rich oxides [61] and, as discussed above, Mercury's crust appears to be very low in Fe^{2+}. The possibility remains, however, that Mercury's crust may contain sufficient metallic iron or iron sulfides [62] to display magnetic thermoremanence and crustal fields detectable from orbit.

A new look at the idea that crustal remanence may give rise to the dipolar field has come from a consideration of the strong variation of solar heating with latitude and longitude on Mercury [63]. Because Mercury's obliquity (the angle that the spin axis makes with the normal to the planet's orbital plane) is small, equatorial regions are heated by the Sun to a greater degree than polar regions. Further, Mercury's eccentric orbit and 3:2 spin–orbit resonance result in two equatorial 'hot poles' that view the Sun at zenith when Mercury is at perihelion (and two equatorial 'cold poles' midway between them). Despite a theorem that a uniform spherical shell magnetized by an internal field displays no external field after the internal field has been removed [64], a result that is not strictly correct when the magnetizing effect of the crustal field is included [65], the thickness of Mercury's crust that is below the Curie temperature of a given magnetic carrier varies spatially [63]. As a result, there is a strong dipolar contribution to the external field that would be produced by a crust magnetized by a past internal field, the predicted dipole moment [63] is within the range of estimates for Mercury [55], and the predicted ratio of quadrupole to dipole terms [63] is testable with future spacecraft measurements.

A hydromagnetic dynamo in a liquid, metallic outer core [56,59] requires both that a substantial fraction of Mercury's core is presently fluid and that there are sufficient sustained sources of heat or chemical buoyancy within the core to drive the convective motions needed to maintain a dynamo. Because it is not known that either requirement is met in Mercury, more exotic dynamo models have been considered. If the fluid outer core is sufficiently thin and the core–mantle boundary is distorted by mantle convective patterns, thermoelectric currents might be driven by temperature differences at the top of the core [66]. A thermoelectric dynamo is likely to produce a field richer in shorter-wavelength harmonics than an Earth-like dynamo, and these harmonics may correlate with those for the gravity field [66], so distinguishing among dynamo models should be possible from orbital measurements.

Recent work on the present state of Mercury's core and its ability to sustain convective motions places new constraints on the range of possible core compositions consistent with an Earth-like convective dynamo. Dynamo simulations carried out as a function of the fractional size of a solid inner core suggest that magnetic field generation becomes difficult in situations where the inner core radius is more than about half the radius of the outer core [67]. Thermal history models [44] indicate that the fractional inner core radius remains less than 0.5 for the lifetime of the planet as long as the core sulfur content is at least 5% by weight. These calculations neglect the contribution of any radioactive or tidal heat generation in the core. New laboratory experiments have reopened the question of whether a significant fraction of potassium in a differentiating terrestrial planet may partition into a liquid metal phase at high pressures [68]. Although potassium is not expected to be abundant on Mercury on the basis of several of the cosmochemical hypotheses for the planet's high metal fraction, potassium derived from the crust is present in the atmosphere and even a small fraction of ^{40}K in the core would have a significant impact on the history of core cooling and the energy available to maintain a core dynamo. Tidal dissipation in the outer core may be important for maintaining a fluid state, but uncertainties in Mercury's internal structure prevent a definitive assessment [69].

Determining the geometry of Mercury's intrinsic magnetic field will elucidate all of these issues. The challenge to such a determination is that external sources can dominate the total measured field at Mercury, as was the situation for Mariner 10 [54]. Errors from external fields were such that the uncertainty in Mercury's dipole moment derived from Mariner 10 data is a factor of 2, and higher-order terms are linearly dependent [55]. Simulations of field recovery from orbital observations to be made by MESSENGER [70] and BepiColombo [71], however, indicate that the effects of the dynamics of the solar wind and Mercury's magnetosphere can be substantially reduced and important aspects of the internal field determined.

5. State of Mercury's core

An observation that can demonstrate the existence and determine the radius of a liquid outer core on Mercury is the measurement of the amplitude of Mercury's forced physical libration [72]. The physical libration of the mantle (manifested as an annual variation in the spin rate about the mean value) is the result of the periodically reversing torque on the planet as Mercury rotates relative to the Sun. The amplitude of this libration ϕ_0 is approximately equal to $(B-A)/C_m$, where A and B are the two equatorial principal moments of inertia of the planet and C_m is the polar moment of inertia of the solid outer part of the planet [72]. The moment differences also appear in expressions for the second-degree coefficients of the planetary gravity field expanded in spherical harmonics. The latter relations, the libration amplitude, and an expression resulting from Mercury's resonant state and relating the planet's small but non-zero obliquity to moment differences and other orbital parameters together yield C_m/C, where C is the polar moment of inertia of the planet [72]. The quantity C_m/C is unity for a completely solid planet and about 0.5 if Mercury has a fluid outer core [72].

Two conditions on the above relationship for ϕ_0 are that the fluid outer core does not follow the 88-day physical libration of the mantle and that the core does follow the mantle on the time scale of the 250 000-year precession of the spin axis [72]. These constraints lead to bounds on the viscosity of outer core material, under the assumption that coupling between the outer core and solid mantle is viscous in nature, but the bounds are so broad as to be readily satisfied. Alternative core–mantle coupling mechanisms, including pressure forces on irregularities in the core–mantle boundary, gravitational torques between the mantle and an axially asymmetric solid inner core, and magnetic coupling between the electrically conductive outer core and a conducting layer at the base of the mantle, do not violate either of the required conditions [73].

Of the four quantities needed to determine whether Mercury has a fluid outer core, two of them – the second-degree coefficients in the planet's gravitational field – can be determined only by tracking a spacecraft near the planet [74]. Two means for determining the remaining two quantities – the obliquity and the forced libration amplitude – from a single orbiting spacecraft have been proposed. One makes use of imaging from a spacecraft with precise pointing knowledge [75], while the other involves repeated sampling of the global topography and gravity fields [76]. The MESSENGER mission will use the latter approach [4]. Mercury's obliquity and libration amplitude can also be determined from Earth-based radar observations, utilizing either multiple images of features on Mercury viewed with a common geometry but at differing times [77] or correlations of the speckle pattern in the radar images obtained at two widely separated antennas [78]. Observations made with the latter method are under way [79].

6. Mercury's polar deposits

The discovery in 1991 of radar-bright regions

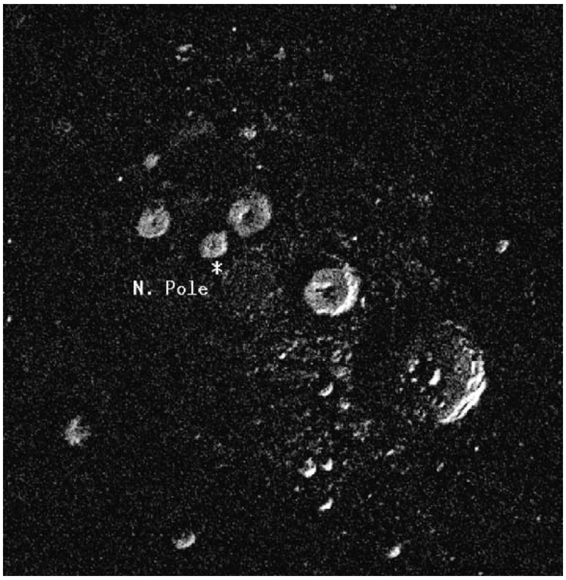

Fig. 7. Radar image of the north polar region of Mercury, obtained by the Arecibo Observatory in July 1999 [82]. The radar illumination direction is from the upper left, and the resolution is 1.5 km. Mercury polar deposits are the radar-bright regions within crater floors.

near Mercury's poles and the similarity of the radar reflectivity and polarization characteristics of these regions to those of icy satellites and the south residual polar cap of Mars led to the proposal that these areas host deposits of surface or near-surface water ice [80,81]. Subsequent radar imaging at improved resolution (Fig. 7) has confirmed that the radar-bright deposits are confined to the floors of near-polar impact craters [82]. Because of the small obliquity of the planet, sufficiently deep craters are permanently shadowed and are predicted to be at temperatures at which water ice is stable for billions of years [83]. Such water ice is not likely to represent exposed portions of larger subsurface polar caps, on the grounds that polar craters display depth-to-diameter ratios similar to those of equatorial craters, contrary to the terrain softening expected in areas of subsurface ice [84]. While a contribution from interior outgassing cannot be excluded, impact volatilization of cometary and meteoritic material followed by random-walk transport of water molecules to polar craters can provide sufficient polar ice to match the characteristics of the deposits [85].

The highest-resolution images of polar deposits show that they extend more than 10° in latitude from the pole and that for larger craters farther from the pole the radar-bright material is concentrated on the side of the crater floor farthest from the pole [82]. Both of these characteristics are consistent with thermal models for water ice insulated by burial beneath a layer of regolith tens of centimeters thick [86], although the detection of radar-bright features in craters as small as 10 km in diameter and the observation that some radar-bright deposits within about 30° of longitude of the equatorial 'cold poles' extend up to 18° southward from the north pole pose difficulties for current thermal models [82].

Two alternative explanations of the radar-bright polar deposits of Mercury have been suggested. One is that the polar deposits are composed of elemental sulfur rather than water ice, on the grounds that sulfur would be stable in polar cold traps and the presence of sulfides in the regolith can account for a high disk-averaged index of refraction and low microwave opacity of surface materials [62]. The second alternative hypothesis is that the permanently shadowed portions of polar craters are radar-bright not because of trapped volatiles but because of either unusual surface roughness [87] or low dielectric loss [88] of near-surface silicates at extremely cold temperatures. This second suggestion can be tested by carrying out impact experiments with very cold silicate targets [87] or measuring dielectric losses of silicates at appropriate temperatures and frequencies [88], while the first proposal can potentially be tested by measurements from an orbiting spacecraft.

Determining the nature of the polar deposits from Mercury orbit will pose a challenge because the deposits will occupy a comparatively small fraction of the viewing area for most remote sensing instruments and because any polar volatiles may be buried beneath a thin layer of regolith. The most promising measurements include searches of the polar atmosphere with an ultraviolet spectrometer for the signature of excess OH or S [89] and neutron spectrometer observations of the polar surface to seek evidence for near-surface hydrogen [32].

7. Mercury's exosphere

Mercury's atmosphere is a surface-bounded exosphere whose composition and behavior are controlled by interactions with the magnetosphere and the surface. The atmosphere is known to contain six elements (H, He, O, Na, K, Ca). The Mariner 10 airglow spectrometer detected H, He, and O [90], while ground-based spectroscopic observations led to the discovery of Na and K [91,92] and more recently Ca [93]. The exosphere is not stable on timescales comparable to the age of the planet, so there must be sources for each of the constituents. H and He are likely to be dominated by solar wind ions neutralized by recombination at the surface, but crustal sources are required for the other species.

Proposed source processes for supplying exospheric species from Mercury's crust include diffusion from the interior, evaporation, sputtering by photons and energetic ions, chemical sputtering by protons, and meteoritic infall and vaporization [90]. That several of these processes play some role is suggested by the strong variations in exospheric characteristics observed as functions of local time, solar distance, and level of solar activity [94–96] as well as by correlations between atmospheric Na and K enhancements and surface features [97]. A recent simulation of Mercury's Na exosphere and its temporal variation in which most of the above source processes were incorporated has shown that evaporation exerts a strong control on the variation of surface Na with time of day and latitude [98]. The simulation provides a good match to measurements of the changes in the Na exosphere with solar distance and time of day [99] and to recent observations [100] of Mercury's sodium tail (Fig. 8).

The presence of the volatile elements Na and K in Mercury's exosphere poses a potential challenge for the hypotheses advanced to account for Mercury's high ratio of metal to silicate. Whether Mercury is metal-rich because of mechanical segregation between metal and silicate grains in the hot, inner solar nebula [16] or because of extensive volatilization or impact removal of the outer portions of a differentiated planet [14,17–19], the planetary crustal concentrations of volatile elements should be very low. For several of the proposed sources of exospheric Na and K, crustal abundances ranging from a few tenths of a percent to a few percent by weight are commonly required [95]. The most recent simulations of the Na exosphere, however, can match all observations with a supply of fresh Na no greater than that predicted by meteoritic impact volatilization [98].

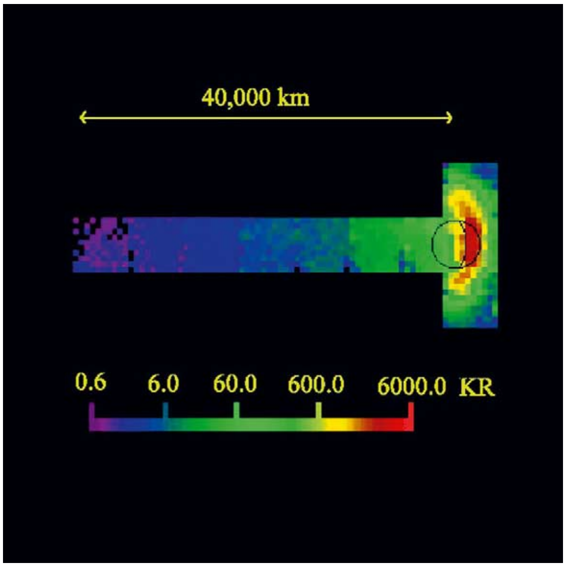

Fig. 8. Composite image of the sodium D_2 emission line in the vicinity of Mercury obtained at the McMath–Pierce Solar Telescope at the National Solar Observatory on 26 May 2001 [100]. The Na tail is in the anti-sunward direction, and south is at the top. The color scale for intensity (in kiloRayleighs) is logarithmic.

A spacecraft in orbit about Mercury will provide a range of opportunities for elucidating further the nature of the exosphere. Limb scans conducted with an ultraviolet-visible spectrometer can monitor variations in the major exospheric constituents and search for new species [33]. Surface sources of exospheric materials can be mapped with γ-ray, X-ray, and neutron spectrometers. Measurement of energetic and thermal plasma ions will detect solar wind pick-up ions that originated as exospheric neutral atoms [101].

8. Concluding discussion

The primary open scientific questions at Mercury are all interconnected. Mercury's composition, beyond providing a test for theories of the planet's formation, controlled the history of volcanism and core cooling and dictates the crustal species capable of transport to the exosphere. Mercury's bombardment flux provided time markers for unraveling the planet's geologic history and delivered key constituents to the surface, including perhaps the polar deposits. The evolution of the core governed the history of magnetic field generation, mantle convection, and contractional tectonics of the crust. Mercury's magnetosphere interacts strongly with the solar wind plasma, the exosphere, and the surface.

The unresolved issues at Mercury also have broad implications for the terrestrial planets as a system. Mercury's composition holds clues to the chemical make-up of the circumsolar nebular disk and to the processes by which planetary embryos interacted and collided to create the final inner planets. Mercury's geological evolution provides an intermediate example, midway between the Moon and Mars, for how planet size governs the history of internal magmatism and deformation. Mercury's core and magnetic field structures, once elucidated, will inform the relationships between cooling and dynamo generation in iron-rich cores. Determining the nature of Mercury's polar deposits and unraveling the myriad connections among Mercury's exosphere, surface, and magnetosphere will sharpen our insight into the behavior of volatiles in the inner solar system.

All of these scientific questions will be addressed by the multiple spacecraft scheduled to encounter Mercury within the coming decade. With the successful completion of the MESSENGER and BepiColombo missions, the innermost planet should be far less enigmatic than at present, and the processes that govern Earth-like planets should be far better understood.

Acknowledgements

I thank John Harmon, Steven Hauck, Andrew Potter, Mark Robinson, and Ann Sprague for generously supplying figures; Paul Butler and Ann Sprague for instructive discussions; Clark Chapman, James Head, Rosemary Killen, Stanton Peale, Emma-Kate Potter, Tilman Spohn, and Ann Sprague for comments on an earlier draft; and Janice Dunlap and Sandra Keiser for assistance with manuscript preparation. Support for this work was provided by the NASA Planetary Geology and Geophysics Program through Grant NAG5-10165 and the NASA Discovery Program through Contract NASW-00002.***[AH]***

References

[1] R.G. Strom, A.L. Sprague, Exploring Mercury: The Iron Planet, Springer, New York, 2003, in press.

[2] G.W. Marcy, R.P. Butler, Planets orbiting other suns, Publ. Astron. Soc. Pacific 112 (2000) 137–140.

[3] S. Seager, The search for extrasolar Earth-like planets, Earth Planet. Sci. Lett. 208 (2003) 113–124.

[4] S.C. Solomon, R.L. McNutt Jr., R.E. Gold, M.H. Acuña, D.N. Baker, W.V. Boynton, C.R. Chapman, A.F. Cheng, G. Gloeckler, J.W. Head III, S.M. Krimigis, W.E. McClintock, S.L. Murchie, S.J. Peale, R.J. Phillips, M.S. Robinson, J.A. Slavin, D.E. Smith, R.G. Strom, J.I. Trombka, M.T. Zuber, The MESSSENGER mission to Mercury: scientific objectives and implementation, Planet. Space Sci. 49 (2001) 1445–1465.

[5] R.E. Gold, S.C. Solomon, R.L. McNutt Jr., A.G. Santo, J.B. Abshire, M.H. Acuña, R.S. Afzal, B.J. Anderson, G.B. Andrews, P.D. Bedini, J. Cain, A.F. Cheng, L.G. Evans, W.C. Feldman, R.B. Follas, G. Gloeckler, J.O. Goldsten, S.E. Hawkins III, N.R. Izenberg, S.E. Jaskulek, E.A. Ketchum, M.R. Lankton, D.A. Lohr, B.H. Mauk, W.E. McClintock, S.L. Murchie, C.E. Schlemm II, D.E. Smith, R.D. Starr, T.H. Zurbuchen, The MESSENGER mission to Mercury: scientific payload, Planet. Space Sci. 49 (2001) 1467–1479.

[6] A.G. Santo, R.E. Gold, R.L. McNutt Jr., S.C. Solomon, C.J. Ercol, R.W. Farquhar, T.J. Hartka, J.E. Jenkins, J.V. McAdams, L.E. Mosher, D.F. Persons, D.A. Artis, R.S. Bokulic, R.F. Conde, G. Dakermanji, M.E. Goss Jr., D.R. Haley, K.J. Heeres, R.H. Maurer, R.C. Moore, E.H. Rodberg, T.G. Stern, S.R. Wiley, B.G. Williams, C.L. Yen, M.R. Peterson, The MESSENGER mission to Mercury: spacecraft and mission design, Planet. Space Sci. 49 (2001) 1481–1500.

[7] R. Grard, A. Balogh, Returns to Mercury: science and mission objectives, Planet. Space Sci. 49 (2001) 1395–1407.

[8] A. Anselmi, G.E.N. Scoon, BepiColombo, ESA's Mercury Cornerstone mission, Planet. Space Sci. 49 (2001) 1409–1420.

[9] M. Novara, The BepiColombo Mercury surface element, Planet. Space Sci. 49 (2001) 1421–1435.

[10] R.L. McNutt, Jr., S.C. Solomon, R. Grard, M. Novara, T. Mukai, An international program for Mercury exploration: synergy of MESSENGER and BepiColombo, Adv. Space Res. (2003) in press.

[11] H. Harder, G. Schubert, Sulfur in Mercury's core?, Icarus 151 (2001) 118–122.

[12] S.J. Weidenschilling, J.N. Cuzzi, Formation of planetesimals in the solar nebula, in: E.H. Levy, J.I. Lunine (Eds.), Protostars and Planets III, University of Arizona Press, Tucson, AZ, 1993, pp. 1031–1060.

[13] S.J. Kortenkamp, E. Kokubo, S.J. Weidenschilling, Formation of planetary embryos, in: R.M. Canup, K. Righter (Eds.), Origin of the Earth and Moon, University of Arizona Press, Tucson, AZ, 2000, pp. 85–100.

[14] G.W. Wetherill, Accumulation of Mercury from planetesimals, in: F. Vilas, C.R. Chapman, M.S. Matthews (Eds.), Mercury, University of Arizona Press, Tucson, AZ, 1988, pp. 670–691.

[15] G.W. Wetherill, Provenance of the terrestrial planets, Geochim. Cosmochim. Acta 58 (1994) 4513–4520.

[16] S.J. Weidenschilling, Iron/silicate fractionation and the origin of Mercury, Icarus 35 (1978) 99–111.

[17] A.G.W. Cameron, The partial volatilization of Mercury, Icarus 64 (1985) 285–294.

[18] B. Fegley Jr., A.G.W. Cameron, A vaporization model for iron/silicate fractionation in the Mercury protoplanet, Earth Planet. Sci. Lett. 82 (1987) 207–222.

[19] W. Benz, W.L. Slattery, A.G.W. Cameron, Collisional stripping of Mercury's atmosphere, Icarus 74 (1988) 516–528.

[20] J.S. Lewis, Origin and composition of Mercury, in: F. Vilas, C.R. Chapman, M.S. Matthews (Eds.), Mercury, University of Arizona Press, Tucson, AZ, 1988, pp. 651–669.

[21] F. Vilas, Mercury: absence of crystalline Fe^{2+} in the regolith, Icarus 64 (1985) 133–138.

[22] D.T. Blewett, P.G. Lucey, B.R. Hawke, G.G. Ling, M.S. Robinson, A comparison of Mercurian reflectance and spectral quantities with those of the Moon, Icarus 129 (1997) 217–231.

[23] T.H. Burbine, T.J. McCoy, L.R. Nittler, G.K. Benedix, E.A. Cloutis, T.L. Dickinson, Spectra of extremely reduced assemblages: implications for Mercury, Meteorit. Planet. Sci. 37 (2002) 1233–1244.

[24] A.L. Sprague, J.P. Emery, K.L. Donaldson, R.W. Russell, D.K. Lynch, A.L. Mazuk, Mercury: mid-infrared (3–13.5 μm) observations show heterogeneous composition, presence of intermediate and basic soil types, and pyroxene, Meteorit. Planet. Sci. 37 (2002) 1255–1268.

[25] D.T. Blewett, B.R. Hawke, P.G. Lucey, Lunar pure anorthosite as a spectral analog for Mercury, Meteorit. Planet. Sci. 37 (2002) 1245–1254.

[26] M.S. Robinson, G.J. Taylor, Ferrous oxide in Mercury's crust and mantle, Meteorit. Planet. Sci. 36 (2001) 841–847.

[27] S.G. Love, K. Keil, Recognizing mercurian meteorites, Meteoritics 30 (1995) 269–278.

[28] A. Yamaguchi, R.N. Clayton, T.K. Mayeda, M. Ebihara, Y. Oura, Y.N. Miura, H. Haramura, K. Misawa, H. Kojima, K. Nagao, A new source of basaltic meteorites inferred from Northwest Africa 011, Science 296 (2002) 334–336.

[29] H. Palme, A new solar system basalt, Science 296 (2002) 271–273.

[30] J. Brückner, J. Masarik, Planetary gamma-ray spectroscopy of the surface of Mercury, Planet. Space Sci. 45 (1997) 39–48.

[31] M. Grande, S.K. Dunkin, B. Kellett, Opportunities for X-ray remote sensing at Mercury, Planet. Space Sci. 49 (2001) 1553–1559.

[32] W.C. Feldman, B.L. Barraclough, C.J. Hansen, A.L. Sprague, The neutron signature of Mercury's volatile polar deposits, J. Geophys. Res. 102 (1997) 25565–25574.

[33] W.E. McClintock, G.M. Holsclaw, The Mercury Atmospheric and Surface Composition Spectrometer (MASCS) for the MErcury Surface, Space ENvironment, GEochemistry, and Ranging (MESSENGER) mission, in: Mercury: Space Environment, Surface, and Interior, Lunar and Planetary Institute, Houston, TX, 2001, p. 62.

[34] S.E. Hawkins, III, J.D. Boldt, E.H. Darlington, M.P. Grey, C.J. Kardian, Jr., S.L. Murchie, K. Peacock, E.D. Schaefer, B.D. Williams, Overview of the MESSENGER Mercury Dual Imaging System, in: Mercury: Space Environment, Surface, and Interior, Lunar and Planetary Institute, Houston, TX, 2001, pp. 42–43.

[35] G. Neukum, J. Oberst, H. Hoffmann, R. Wagner, B.A. Ivanov, Geologic evolution and cratering history of Mercury, Planet. Space Sci. 49 (2001) 1507–1521.

[36] M.T. Zuber, S.C. Solomon, R.J. Phillips, D.E. Smith, G.L. Tyler, O. Aharonson, G. Balmino, W.B. Banerdt, J.W. Head, C.L. Johnson, F.G. Lemoine, P.J. McGovern, G.A. Neumann, D.D. Rowlands, S. Zhong, Internal structure and early thermal evolution of Mars from Mars Global Surveyor topography and gravity, Science 287 (2000) 1788–1793.

[37] P.J. McGovern, S.C. Solomon, D.E. Smith, M.T. Zuber, G. Simons, R.J. Wieczorek, R.J. Phillips, G.A. Neumann, O. Aharonson, J.W. Head, Localized gravity/topography admittance and correlation spectra on Mars: implications for regional and global evolution, J. Geophys. Res. 107 (E12) (2002) 10.1029/2001JE001854.

[38] F. Nimmo, Constraining the crustal thickness on Mercury from viscous topographic relaxation, Geophys. Res. Lett. 29 (5) (2002) 10.1029/2001GL013883.

[39] R.G. Strom, Mercury: an overview, Adv. Space Res. 19 (1997) 1471–1485.

[40] S.M. Milkovich, J.W. Head, L. Wilson, Identification of mercurian volcanism: resolution effects and implications for MESSENGER, Meteorit. Planet. Sci. 37 (2002) 1209–1222.

[41] R. Jeanloz, D.L. Mitchell, A.L. Sprague, I. de Pater, Evi-

dence for a basalt-free surface on Mercury and implications for internal heat, Science 268 (1995) 1455–1457.
[42] M.S. Robinson, P.G. Lucey, Recalibrated Mariner 10 color mosaics: implications for mercurian volcanism, Science 275 (1997) 197–198.
[43] T.R. Watters, M.S. Robinson, A.C. Cook, Topography of lobate scarps on Mercury: new constraints on the planet's contraction, Geology 26 (1998) 991–994.
[44] S.A. Hauck, II, A.J. Dombard, R.J. Phillips, S.C. Solomon, Internal and tectonic evolution of Mercury, Earth Planet. Sci. Lett. (2003) submitted.
[45] A.J. Dombard, S.A. Hauck, II, S.C. Solomon, R.J. Phillips, Potential for long-wavelength folding on Mercury, Lunar Planet. Sci. 32 (2001) abstract 2035 (CD-ROM).
[46] T.R. Watters, R.A. Schultz, M.S. Robinson, A.C. Cook, The mechanical and thermal structure of Mercury's early lithosphere, Geophys. Res. Lett. 29 (11) (2002) 10.1029/2001GL014308.
[47] R.F. Dantowitz, S.W. Teare, M.J. Kozubal, Ground-based high-resolution imaging of Mercury, Astron. J. 119 (2000) 2455–2457.
[48] J. Baumgardner, M. Mendillo, J.K. Wilson, A digital high-definition imaging system for spectral studies of extended planetary atmospheres. I. Initial results in white light showing features on the hemisphere of Mercury unimaged by Mariner 10, Astron. J. 119 (2000) 2458–2464.
[49] J. Warell, S.S. Limaye, Properties of the Hermean regolith: I. Global regolith albedo variation at 200 km scale from multicolor CCD imaging, Planet. Space Sci. 49 (2001) 1531–1552.
[50] M. Mendillo, J. Warell, S.S. Limaye, J. Baumgardner, A. Sprague, J.K. Wilson, Imaging of Mercury using ground-based telescopes, Planet. Space Sci. 49 (2001) 1501–1505.
[51] J.K. Harmon, Mercury radar studies and lunar comparisons, Adv. Space Res. 19 (1997) 1487–1496.
[52] J.K. Harmon, Mercury radar imaging at Arecibo in 2001, Lunar Planet. Sci. 33 (2002) abstract 1858 (CD-ROM).
[53] A.C. Cook, M.S. Robinson, Mariner 10 stereo image coverage of Mercury, J. Geophys. Res. 105 (2000) 9429–9443.
[54] N.F. Ness, K.W. Behannon, R.P. Lepping, Y.C. Whang, Observations of Mercury's magnetic field, Icarus 28 (1976) 479–488.
[55] J.E.P. Connerney, N.F. Ness, Mercury's magnetic field and interior, in: F. Vilas, C.R. Chapman, M.S. Matthews (Eds.), Mercury, University of Arizona Press, Tucson, AZ, 1988, pp. 494–513.
[56] D.J. Stevenson, Planetary magnetic fields, Earth Planet. Sci. Lett. 208 (2003) 1–11.
[57] A. Stephenson, Crustal remanence and the magnetic moment of Mercury, Earth Planet. Sci. Lett. 28 (1976) 454–458.
[58] L.J. Srnka, Magnetic dipole moment of a spherical shell with TRM acquired in a field of internal origin, Phys. Earth Planet. Inter. 11 (1976) 184–190.
[59] G. Schubert, M.N. Ross, D.J. Stevenson, T. Spohn, Mercury's thermal history and the generation of its magnetic field, in: F. Vilas, C.R. Chapman, M.S. Matthews (Eds.), Mercury, University of Arizona Press, Tucson, AZ, 1988, pp. 429–460.
[60] M.H. Acuña, J.E.P. Connerney, N.F. Ness, R.P. Lin, D. Mitchell, C.W. Carlson, J. McFadden, K.A. Anderson, H. Rème, C. Mazelle, D. Vignes, P. Wasilewski, P. Cloutier, Global distribution of crustal magnetization discovered by the Mars Global Surveyor MAG/ER experiment, Science 284 (1999) 790–793.
[61] G. Kletetschka, P. Wasilewski, P.T. Taylor, Mineralogy of the sources for magnetic anomalies on Mars, Meteorit. Planet. Sci. 35 (2000) 895–899.
[62] A.L. Sprague, D.M. Hunten, K. Lodders, Sulfur at Mercury, elemental at the poles and sulfides in the regolith, Icarus 118 (1995) 211–215.
[63] O. Aharonson, M.T. Zuber, S.C. Solomon, Crustal remanence in an internally magnetized non-uniform shell: a possible source for Mercury's magnetic field? Earth Planet. Sci. Lett. (2003) in press.
[64] S.K. Runcorn, An ancient lunar magnetic field, Nature 253 (1975) 701–703.
[65] V. Lesur, A. Jackson, Exact solutions for internally induced magnetization in a shell, Geophys. J. Int. 140 (2000) 453–459.
[66] G. Giampieri, A. Balogh, Mercury's thermoelectric dynamo revisited, Planet. Space Sci. 50 (2002) 757–762.
[67] J.M. Aurnou, F. Al-Shamali, M. Heimpel, Dynamo processes in a thin shell geometry, Eos, Trans. AGU 82, Fall Meeting suppl. (2001) F329.
[68] V.R. Murthy, W. van Westrenen, Y. Fei, Experimental evidence that potassium is a substantial radioactive heat source in planetary cores, Nature 423 (2003) 163–165.
[69] B.G. Bills, Tidal dissipation in Mercury, Lunar Planet. Sci. 33 (2002) abstract 1599 (CD-ROM).
[70] H. Korth, B.J. Anderson, R.L. McNutt, Jr., M.H. Acuña, J.A. Slavin, N.A. Tsyganenko, S.C. Solomon, Determination of the properties of Mercury's magnetic field by the MESSENGER mission, Planet. Space Sci. (2003) in press.
[71] G. Giampieri, A. Balogh, Modelling of magnetic field measurements at Mercury, Planet. Space Sci. 49 (2001) 1637–1642.
[72] S.J. Peale, The rotational dynamics of Mercury and the state of its core, in: F. Vilas, C.R. Chapman, M.S. Matthews (Eds.), Mercury, University of Arizona Press, Tucson, AZ, 1988, pp. 461–493.
[73] S.J. Peale, R.J. Phillips, S.C. Solomon, D.E. Smith, M.T. Zuber, A procedure for determining the nature of Mercury's core, Meteorit. Planet. Sci. 37 (2002) 1269–1283.
[74] J.D. Anderson, G. Colombo, P.B. Esposito, E.L. Lau, G.B. Trager, The mass, gravity field, and ephemeris of Mercury, Icarus 71 (1987) 337–349.
[75] X. Wu, P.L. Bender, S.J. Peale, G.W. Rosborough, M.A. Vincent, Determination of Mercury's 88-day libration and fluid core size from orbit, Planet. Space Sci. 45 (1997) 15–19.
[76] D.E. Smith, M.T. Zuber, S.J. Peale, R.J. Phillips, S.C. Solomon, Estimating the libration of Mercury by remote

sensing of gravity and altimetry, in: Mercury: Space Environment, Surface, and Interior, Lunar and Planetary Institute, Houston, TX, 2001, pp. 90–91.
[77] M.A. Slade, R.F. Jurgens, J.-L. Margot, E.M. Standish, Repeat-orbit interferometric precision measurement of Mercury obliquity, in: Mercury: Space Environment, Surface, and Interior, Lunar and Planetary Institute, Houston, TX, 2001, pp. 88–89.
[78] I.V. Holin, Earth-based U.S. opportunities to solve the problem of Mercury's obliquity and librations in May-June 2002, Lunar Planet. Sci. 33 (2002) abstract 1387 (CD-ROM).
[79] J.-L. Margot, S. Peale, R. Jurgens, M. Slade, I. Holin, Mercury interior properties from measurements of librations, in: Abstract Volume, International Astronomical Union 25th General Assembly, Sydney, Australia, 2003, p. 155.
[80] J.K. Harmon, M.A. Slade, Radar mapping of Mercury: full-disk images and polar anomalies, Science 258 (1992) 640–642.
[81] M.A. Slade, R.P. Butler, D.O. Muhleman, Mercury radar imaging: evidence for polar ice, Science 258 (1992) 635–640.
[82] J.K. Harmon, P.J. Perillat, M.A. Slade, High-resolution radar imaging of Mercury's north pole, Icarus 149 (2001) 1–15.
[83] D.A. Paige, S.E. Wood, A.R. Vasavada, The internal stability of water ice at the poles of Mercury, Science 258 (1992) 643–646.
[84] N.G. Barlow, R.A. Allen, F. Vilas, Mercurian impact craters: implications for polar ground ice, Icarus 141 (1999) 194–204.
[85] J.I. Moses, K. Rawlins, K. Zahnle, L. Dones, External sources of water for Mercury's putative ice deposits, Icarus 137 (1999) 197–221.
[86] A.R. Vasavada, D.A. Paige, S.E. Wood, Near-surface temperatures on Mercury and the Moon, Icarus 141 (1999) 179–193.
[87] S.J. Weidenschilling, Mercury's polar radar anomalies: ice and/or cold rock? Lunar Planet. Sci. 29 (1998) abstract 1278 (CD-ROM).
[88] L.V. Starukhina, High radar response of Mercury polar regions: water ice or cold silicates? Lunar Planet. Sci. 31 (2000) abstract 1301 (CD-ROM).
[89] R.M. Killen, J. Benkhoff, T.H. Morgan, Mercury's polar caps and the generation of an OH exosphere, Icarus 125 (1997) 195–211.
[90] R.M. Killen, W.-H. Ip, The surface-bounded atmospheres of Mercury and the Moon, Rev. Geophys. 37 (1999) 361–406.
[91] A.E. Potter, T.H. Morgan, Discovery of sodium in the atmosphere of Mercury, Science 229 (1985) 651–653.
[92] A.E. Potter, T.H. Morgan, Potassium in the atmosphere of Mercury, Icarus 67 (1986) 336–340.
[93] T.A. Bida, R.M. Killen, T.H. Morgan, Discovery of calcium in Mercury's atmosphere, Nature 404 (2000) 159–161.
[94] A.E. Potter, R.M. Killen, T.H. Morgan, Rapid changes in the sodium exosphere of Mercury, Planet. Space Sci. 47 (1999) 1441–1448.
[95] R.M. Killen, A.E. Potter, P. Reiff, M. Sarantos, B.V. Jackson, P. Hick, B. Giles, Evidence for space weather at Mercury, J. Geophys. Res. 106 (2001) 20509–20525.
[96] D.M. Hunten, A.L. Sprague, Diurnal variation of sodium and potassium at Mercury, Meteorit. Planet. Sci. 37 (2002) 1191–1195.
[97] A.L. Sprague, W.J. Schmitt, R.E. Hill, Mercury: sodium atmospheric enhancements, radar-bright spots, and visible surface features, Icarus 136 (1998) 60–68.
[98] F. Leblanc, R.E. Johnson, Mercury's sodium exosphere, Icarus 164 (2003) 261–281.
[99] A.L. Sprague, R.W.H. Kozlowski, D.M. Hunten, N.M. Schneider, D.L. Domingue, W.K. Wells, W. Schmitt, U. Fink, Distribution of abundance of sodium in Mercury's atmosphere, 1985–1988, Icarus 129 (1997) 506–527.
[100] A.E. Potter, R.M. Killen, T.H. Morgan, The sodium tail of Mercury, Meteorit. Planet. Sci. 37 (2002) 1165–1172.
[101] P.L. Koehn, T.H. Zurbuchen, G. Gloeckler, R.A. Lundgren, L.A. Fisk, Measuring the plasma environment at Mercury: the fast imaging plasma spectrometer, Meteorit. Planet. Sci. 37 (2002) 1173–1189.
[102] M.S. Robinson, M.E. Davies, T.R. Colvin, K. Edwards, A revised control network for Mercury, J. Geophys. Res. 104 (1999) 30847–30852.
[103] G.W. Marcy, S.S. Vogt, D.A. Fischer, C. McCarthy, R.P. Butler, California and Carnegie Planet Search, 2003, http://exoplanets.org/almanacframe.html.

Sean C. Solomon, Director of the Department of Terrestrial Magnetism at the Carnegie Institution of Washington, is the Principal Investigator for the MESSENGER mission to Mercury. Educated at Caltech and M.I.T., he was a member of the M.I.T. faculty for more than 20 years. A seismologist and planetary geophysicist, he served on the science teams of the Magellan mission to Venus and the Mars Global Surveyor mission, and he is a former President of the American Geophysical Union.